

Sequencing and Identification of Endogenous Neuropeptides with Matrix-Enhanced Secondary Ion Mass Spectrometry Tandem Mass Spectrometry

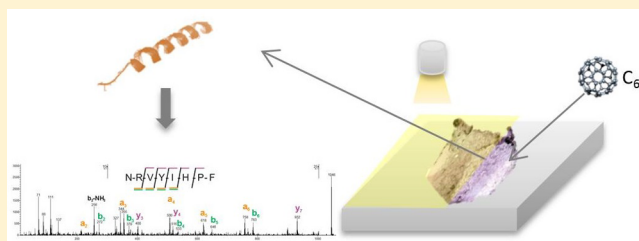
Nina Ogrinc Potočnik,[†] Gregory L. Fisher,[‡] Arnoud Prop,[†] and Ron M. A. Heeren^{*,†}

[†]Maastricht MultiModal Molecular Imaging (M4I) Institute, Division of Imaging Mass Spectrometry, Maastricht University, Maastricht, 6229 ER, The Netherlands

[‡]Physical Electronics Inc., Chanhassen, Minnesota 55317, United States

S Supporting Information

ABSTRACT: Matrix-enhanced secondary ion mass spectrometry (ME-SIMS) has overcome one of the biggest disadvantages of SIMS analysis by providing the ability to detect intact biomolecules at high spatial resolution. By increasing ionization efficiency and minimizing primary ion beam-induced fragmentation of analytes, ME-SIMS has proven useful for detection of numerous biorelevant species, now including peptides. We report here the first demonstration of tandem ME-SIMS for de novo sequencing of endogenous neuropeptides from tissue in situ (i.e., rat pituitary gland). The peptide ions were isolated for tandem MS analysis using a 1 Da mass isolation window, followed by collision-induced dissociation (CID) at 1.5 keV in a collision cell filled with argon gas, for confident identification of the detected peptide. Using this method, neuropeptides up to m/z 2000 were detected and sequenced from the posterior lobe of the rat pituitary gland. These results demonstrate the potential for ME-SIMS tandem MS development in bottom-up proteomics imaging at high-spatial resolution.



Secondary ion mass spectrometry (SIMS), one of the oldest MSI techniques, has become increasingly popular for the analysis of biologically relevant samples, due in part to its capacity to obtain chemical and spatial information at unmatched lateral resolutions. SIMS ability to spatially resolve analytes at such fine lateral resolution is enabled using ion beams that can be focused down to the nanometer scale, which facilitates desorption and ionization of surface molecules at such spatial scales accordingly. This spatial resolution is superior to diffraction-limited laser-based MS approaches, such as matrix-assisted laser desorption/ionization (MALDI). However, the excessive energy of the primary ions limits the method to the detection of elements, fragmented molecules, and small ($\leq m/z$ 1000) intact molecular species for nearly all practical purposes.^{1,2} Consequently, SIMS is restricted in its ability to ionize and detect large intact molecular species, such as peptides and proteins, with high sensitivity.

Matrix-enhanced secondary ion mass spectrometry (ME-SIMS) has demonstrated an increase in the ionization efficiency of intact molecules such as lipids and peptides. Last year marked the 20th anniversary of the first ME-SIMS experiment performed by Wu and Odom³ showing the ability to detect protein species up to 10 kDa. The SIMS community explored the ionization efficiency and mechanisms of different organic matrices commonly used for MALDI analysis,^{4,5} reactive matrices,⁶ and ionic liquid matrices^{7,8} in SIMS-based endeavors. In the past, the use of ME-SIMS was limited to standards and extracts due to distortion of spatial resolution and delocaliza-

tion of analytes caused by the typical techniques used for matrix application. Specifically, the crystal size of the matrix ultimately dictates the maximum attainable lateral resolution, as analyte migration from the sample's surface occurs over such area during the analyte extraction and matrix crystal formation. In other words, if the matrix application creates large, inhomogeneous crystalline structures, then the ability to confidently localize an analyte within an area is diminished. New advances in sample preparation techniques, such as sublimation devices and automated spray systems, allow researchers to control the homogeneity of the matrix and crystal size and minimize the delocalization of molecular species.

Time-of-flight (TOF) analyzers typically lack sufficient mass resolution or capabilities to separate and identify isobaric species. Instrument innovations, such as the introduction of a parallel imaging tandem MS spectrometer on a TOF-SIMS platform,⁹ C₆₀ source coupled to the FTICR spectrometer,^{10,11} and new hybrid SIMS system fused to an Orbitrap spectrometer, now separate isobaric compounds and identify them at high spatial resolution. These recent innovations enable new applications of high-resolution SIMS in peptidomics and other fields.

Received: July 3, 2017

Accepted: July 28, 2017

Published: July 28, 2017

Peptide sequencing has been an unexplored domain in SIMS for two reasons. First, only few tandem MS-enabled SIMS instruments were available. Second, the desorption and ionization of intact peptide species directly from tissue sections were near to impossible with conventional SIMS approaches. Though a trivial matter in MALDI, where peptide sequencing has been used to study various diseases, the extraction of peptide species is limited in SIMS due to intense fragmentation caused by energetic primary ion particles. Several sequencing attempts have been made by looking at the fragmentation pattern in MS¹ from digested proteins with¹² or without¹³ prior liquid chromatography steps with LC-ME-SIMS. A sequencing study of biodevices¹⁴ with Ar clusters as “soft-ionization” source was limited to the identification of a single peptide. Here, we show, using ME-SIMS sample preparation and TOF-SIMS tandem MS, the capability of performing peptide sequencing on extracted, intact endogenous peptides directly from tissue and with limited spatial distortion and migration of analytes. This experimental setup shows for the first time a new application for peptidomics by SIMS tandem MS with the potential for high-resolution imaging.

EXPERIMENTAL SECTION

Bruker Peptide Mix Standard Solutions. Solutions of the Bruker peptide standard mix II (Bruker GmbH, Bremen, Germany) consisting of Bradykinin 1-7 (*m/z* 757), Angiotensin II (*m/z* 1046) and I (*m/z* 1296), Substance P (*m/z* 1347), Bombesin (*m/z* 1619), ACTH clip 1-17 (*m/z* 2093), ACTH clip 18-39 (*m/z* 2465), and Somatostatin (*m/z* 2093) were spotted on doped Si-wafers (Siltronix, Archamps, France) in 1:1 ratio of the peptide mix and 7 mg/mL α -cyano-4-hydroxycinnamic acid (CHCA, Sigma-Aldrich, St. Louis, MO, USA) in 50% acetonitrile (ACN, Biosolve, Valkenswaard, Netherlands) and 1% trifluoroacetic acid (TFA; Sigma-Aldrich, St. Louis, MO, USA). The droplet was left to dry prior to analysis.

Sample Preparation. Fresh frozen pituitary glands from Wistar HAN rats were sectioned with 12 μ m thicknesses using a cryo-microtome (HMS25, MICROM, Walldorf Germany), thaw-mounted on indium tin oxide (ITO) glass slides (Delta Technologies, Loveland, CO, USA), and stored at -80°C until further analysis. Prior to analysis, the samples were consecutively dipped in iced-cold CHCl_3 (Sigma-Aldrich, St. Louis, MO, USA), MeOH (Biosolve, Valkenswaard, Netherlands), and EtOH (Biosolve, Valkenswaard, Netherlands) for 30 s, 30 s, and 1 min, respectively. Washed tissues were then coated with CHCA (7 mg/mL 50% ACN, 0.2% TFA) using a TM-sprayer (HTX technologies, Carboro, NC, USA), using two passes at 80°C , 0.1 mL/min flow rate, 10 psi spray pressure, 2 mm spray spacing, 1200 mm/min spray velocity, and 40 mm sprayer nozzle distance to sample.

SIMS Imaging. All TOF-SIMS tandem MS analyses were performed using a PHI *nanoTOF* II instrument (Physical Electronics, Chanhassen, MN, USA) with either a 60 keV Bi_3^{2+} or a 20 keV C_{60}^+ cluster ion gun for tandem MS imaging experiments.⁹ The beam diameter of the 20 keV C_{60}^+ was $\sim 5 \mu\text{m}$ measured using a calibrated tuning grid. The analytical field-of-view (FOV) was in $100 \mu\text{m} \times 100 \mu\text{m}$ with 256 pixels \times 256 pixels for Bruker peptide mix solutions, resulting in a $0.4 \mu\text{m}$ pixel size, and $600 \mu\text{m} \times 600 \mu\text{m}$ with 512 pixels \times 512 pixels for tissue imaging, resulting in a $1.2 \mu\text{m}$ pixel size. The sample dose was in all cases at or below the static limit (10^{13} ions cm^{-2}). The sample bias was set at 3 kV. The TOF-SIMS

(MS¹) and tandem MS (MS²) data were collected simultaneously in positive ion polarity as described in Fisher et al.⁹ The tandem MS experiments were performed using 1.5 keV collision-induced dissociation (CID) with Ar gas estimated to be 1×10^{-3} Pa in the collision cell.⁹ In the course of each acquisition, mass spectral information at each image pixel was collected in the range of 0–3000 *m/z* and saved into a raw data stream file. The calibration was performed on low mass identified peptide fragments.

Data Analysis. The images and spectral data were processed using PHI SmartSoft-TOF and PHI TOF-DR (Physical Electronics, Chanhassen, MN, USA) software. Except for intensity scaling and convolution, no additional data processing was applied. The MS² fragmentation spectra were compared to the online sequence database Protein Prospector,¹⁵ and the fragments were putatively assigned accordingly.

Scanning Electron Microscopy (SEM) Imaging. After analysis, the samples were analyzed using a 10-keV scanning electron microscope (XL-30, Philips, The Netherlands) to determine the coverage and the produced crystal size after matrix application. Sections were gold-coated with the sputter coater (108 Auto, Cressington, UK), and images were taken at 100 \times (Figure 1b), 8000 \times (Figure 1c), and 10 000 \times (Figure 1d) magnification.

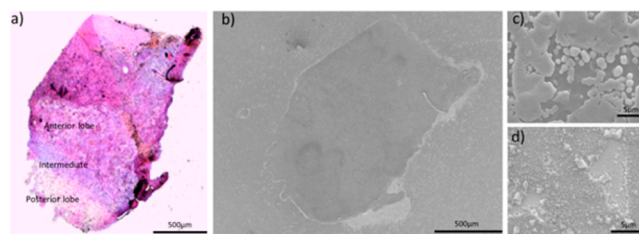


Figure 1. Optical images of the pituitary gland post-SIMS measurements. (a) H&E-stained pituitary gland with the anterior, intermediate, and posterior lobes labeled. (b–d) SEM images at 100 \times (b), 8000 \times (c), and 10 000 \times (d) magnification. The sizes of the matrix crystals were $\sim 2 \mu\text{m}$ on-tissue (c) and 0.5 – $1 \mu\text{m}$ off-tissue (d).

Hematoxylin and Eosin Staining. In order to identify different features of the pituitary gland, the samples were stained with the following H&E protocol: The section was consecutively dipped in solutions of ethanol (100%, 96%, 96%, 70%, 70%, each for 3 min), in hematoxylin (Merck, Darmstadt, Germany) for 3 min, washed for 3 min under running tap water, dipped in eosin (J.T. Baker, Center Valley, PA, USA) for 30 s, washed for 1 min under warm tap water, and dipped in 100% EtOH for 1 min. The dried images were optically scanned with the MIRAX Desk Scanner (Zeiss, Göttingen, Germany) and annotated accordingly (Figure 1a).

RESULTS AND DISCUSSION

Peptide Sequencing on a Standard. In order to evaluate the peptide sequencing possibilities with the new parallel tandem MS system, we first performed ME-SIMS experiments on a peptide standard (a Bruker peptide mix II) comprised of Bradykinin 1-7 (*m/z* 757), Angiotensin II (*m/z* 1046) and I (*m/z* 1296), Substance P (*m/z* 1347), Bombesin (*m/z* 1619), ACTH clip 1-17 (*m/z* 2093), ACTH clip 18-39 (*m/z* 2465), and Somatostatin (*m/z* 2093). Similar measurements, without tandem MS, were already performed by Svava et al.⁶ to optimize the extraction of peptides using different reactive matrices. In

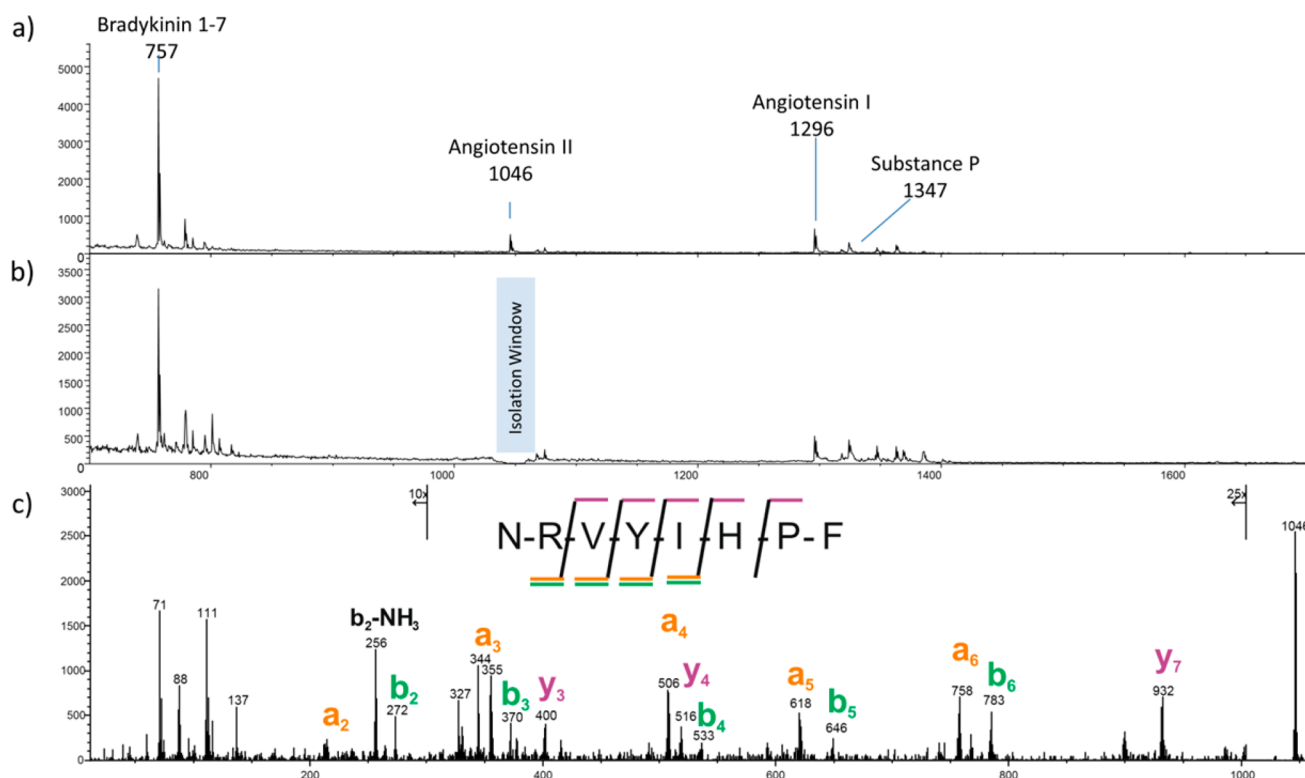


Figure 2. (a) ME-SIMS mass spectrum of the Bruker peptide mix II at the mass range of 700–1700 acquired before the precursor ion selection with annotated peptides and corresponding distribution images. (b) SIMS mass spectrum (MS^1) of the Bruker peptide mix II acquired with the $[M + H]^+$ precursor ion selection of Angiotensin II (m/z 1046). While the precursor selection is monoisotopic, a range of approximately ± 10 Da on either side of the selection window is disturbed. (c) MS^2 spectrum produced by CID and acquired simultaneously with spectrum (b) of the $[M + H]^+$ precursor of Angiotensin II (m/z 1046) with annotation of the major a, b, and y fragment ions.

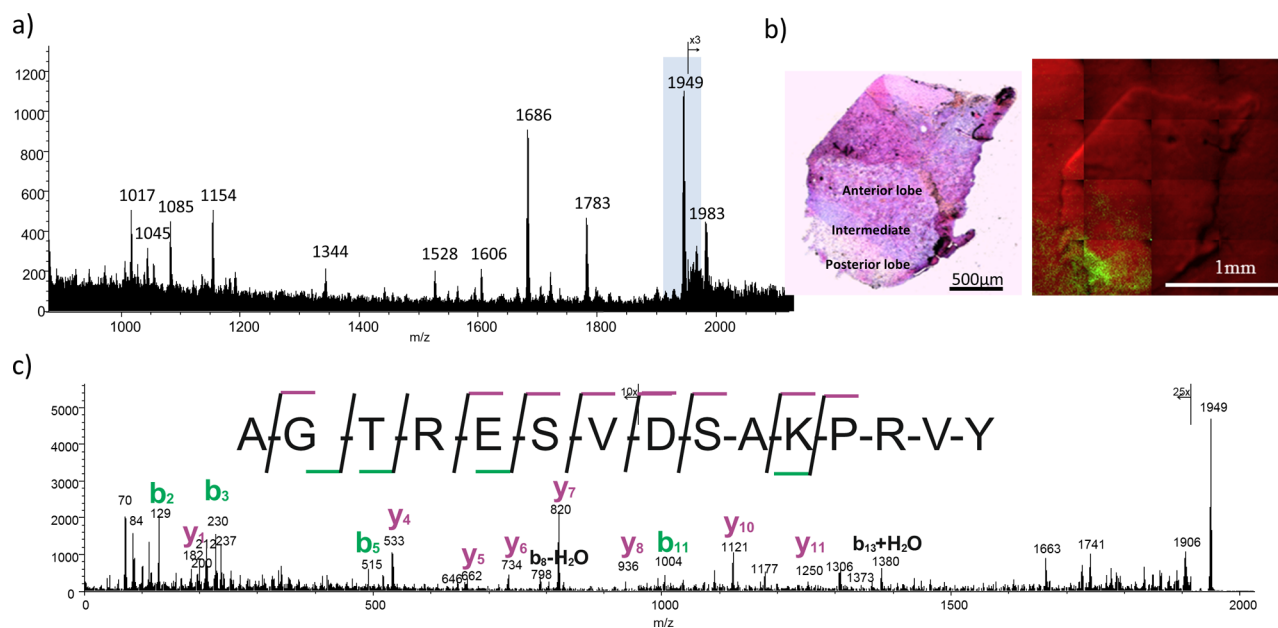


Figure 3. (a) MS^1 ME-SIMS spectrum of extracted endogenous peptides from the pituitary gland. The highlighted (blue) mass m/z 1949 was selected as the precursor ion. (b) H&E-stained image (left) with annotated regions of the pituitary gland and an overlaid SIMS image (right) of the TIC (red) and MS^2 image of the precursor ion (green). (c) MS^2 spectrum produced by CID of the $[M + H]^+$ precursor of m/z 1949 with annotation of the major b and y fragment ions and database identified as AVP_NPII copeptin fragment.

this case, CHCA seemed to be the most promising matrix for peptide extraction. CHCA causes peptide protonation, which increases the intact molecular signal⁷ and is stable under high vacuum, which makes it a suitable candidate for ME-SIMS.

The extracted ME-SIMS peptide spectrum from the standard (Figure 2a) shows the presence of Bradykinin 1-7 (m/z 757), Angiotensin II (m/z 1046) and I (m/z 1296), and Substance P (m/z 1347) with intensities up to 5000 counts. Higher mass

peptides above m/z 2000 were not observed under these conditions. The MS¹ spectrum after the precursor mass selection (in this case m/z 1046) with the approximately 1 Da isolation window⁹ (Figure 2b) shows the advantage of simultaneous collection of MS¹ and MS² spectra. The biggest advantage is the fact that the MS¹ information is not discarded in the course of collecting the MS² product ion data.

Every single intact peptide ion in the MS¹ spectrum was isolated and fragmented with high-energy CID. The fragmentation spectra can be found in the [Supporting Information](#). An example fragmentation spectrum of Angiotensin II (Figure 2c) shows substantial coverage of the sequence by a, b, and y fragments. In comparison, the low-energy CID of peptide precursor ions consist mainly of b and y fragments.¹⁶ The presence of additional fragments demonstrates that ME-SIMS can be employed for peptide sequencing, and de novo identification of each species delivers substantial sequence coverage.

Extraction and Peptide Sequencing of Endogenous Neuropeptides Directly from Pituitary Gland Tissue.

Endogenous neuropeptides are a complex set of messengers controlling a wide variety of regulatory functions in the brain and the central nervous system. They have an important role in many physiological and neurological disease-related processes such as in Alzheimer's and Usher's diseases.^{17–21} These closely related neuropeptides are secreted by smaller organs such as the hypothalamus and pituitary gland and often differ by only a single amino acid. Within these small organs, it is important to differentiate and localize endogenous neuropeptides on the cellular level.

The pituitary gland is a small, neuropeptide-forming and -secreting organ. Neuropeptides are formed in vivo by proteolytic cleavage of proteins at specific cleavage sites and, then, subsequently undergo a variety of posttranslational modifications to activate their biological function. The pituitary gland consists of three different regions formed of glial cells and nerve endings. Each of the areas secretes different prohormones (such as OT_NPI, AVP_NPII, and POMC). The endogenous peptides secreted by different areas of the pituitary gland have already been intensively studied by MALDI-MSI,^{17–19} making it an ideal model for peptide sequencing and comparison with ME-SIMS tandem MS analysis.

We carefully modified the sample preparation protocol in an effort to optimize the extraction of endogenous peptides. Sections were gently washed prior to matrix application in order to remove the salts and reduce the lipid content within the tissue. Only two layers of matrix were applied on the tissue before analysis. The extracted peptides (Figure 3a) are predominantly found in the mass range of 900–2000 Da. A higher number of spectral counts for the extracted peptides were observed in the posterior lobe of the pituitary gland (Figure 3b), where OT_NPI cleaves into single peptide, oxytocin–neurophysin I, and where AVP_NPII is viewed as the signal peptide, vasopressin–neurophysin II–copeptin.¹⁸ The prohormone POMC peptides secreted from the intermediate lobe are typically more acidic, which is why they are more readily observed by MALDI imaging. In our experiment, two of the POMC peptides were extracted and sequenced from the tissue section. In addition, most of the Na/K cationized peptides formed are known to be more difficult to fragment in CID.

Several parent ions locally desorbed and ionized from the smaller area of the pituitary gland were subjected to tandem MS

analysis to determine their molecular identity (Table S1). For example, the MS² spectrum of the extracted precursor at m/z 1949 shows b and y fragments with extensive sequence coverage (Figure 3c). We observed uniform sensitivity of sequence fragments over the entire detected mass range, a benefit over using conventional Fourier transform (FT)-based instrumentation, which can restrict proper peptide identification.¹⁸ Using the Protein Prospector database, the extracted peptide was identified as the AVP_NP II copeptin fragment. Some of the selected precursor ions were detected as potassium adducts of the molecular species, such as oxytocin ($m/z = 1045 [M + K]^+$), resulting in a high intensity of the potassium fragment ion, and thus limited our ability to properly identify the peptide species (tandem MS spectrum can be found in Figure S1). Additional POMC precursor ion peptides were only tentatively assigned to m/z 1686 and m/z 1884 due to a low coverage of the sequence. The mass m/z 1686 most likely corresponds to a fragment of the joining peptide (J-peptide) with identified fragments b5, b9, b16+H₂O, and y16-NH₃ (Figure S2). In the case of the m/z 1884 precursor ion, two different peptides were potentially extracted from the imaged area. They could be assigned to either the (POMC) J-peptide with identified fragments [MH – NH₃], b5-H₂O, y7, y9, y16-NH₃, and x17 or the (POMC) CLIP peptide with identified fragments y3, y15, y16, and b13-H₂O (Figure S3).

CONCLUSION

In this work, we leveraged the advantages of ME-SIMS, which affords increased ionization efficiency and ease of detection of intact molecular species in comparison to traditional SIMS methodologies. The capability of performing parallel tandem MS analysis enables the detection and de novo sequencing of endogenous peptides up to m/z 2000 directly from pituitary gland tissue sections. The platform described demonstrates the ability to perform sequencing without the need of prior chromatographic separation, while providing uniform sensitivity of fragmented ions over the entire detected mass range. We assigned endogenous peptides secreted from the posterior lobe and also tentatively assigned peptide sequences to acidic POMC-cleaved peptides, which are usually only observed with MALDI. In combination with other MSI techniques, this method can elucidate the distribution of endogenous and/or tryptically digested peptides for preclinical studies with the potential for imaging at cellular length scales. Our studies demonstrate that this method can be applied to study disease pathogenesis, for which localization and identification of peptides are needed at significantly greater spatial resolution than can be provided by MALDI imaging.

ASSOCIATED CONTENT

Supporting Information

The Supporting Information is available free of charge on the ACS Publications website at DOI: [10.1021/acs.analchem.7b02573](https://doi.org/10.1021/acs.analchem.7b02573).

Extracted and identified neuropeptides from the pituitary gland; ME-SIMS fragmentation spectra (PDF)

AUTHOR INFORMATION

Corresponding Author

*E-mail: r.heeren@maastrichtuniversity.nl.

ORCID

Gregory L. Fisher: [0000-0001-7517-0512](https://orcid.org/0000-0001-7517-0512)

Ron M. A. Heeren: 0000-0002-6533-7179

Notes

The authors declare no competing financial interest.

ACKNOWLEDGMENTS

The work is part of the LINK program which is financially supported by the Dutch Province of Limburg. N.O.P. acknowledges support from FP7 European Union Marie Curie IAPP Program, BrainPath (PIAPP-GA-2013-612360). We gratefully acknowledge Audrey Jongen (General Surgery, MUMC+) for providing us with the rat pituitary glands and Dr. Christopher Anderton (EMSL-PNNL) for his careful reading of the manuscript.

REFERENCES

- (1) Bolbach, G.; Viari, A.; Galera, R.; Brunot, A.; Blais, J. C. *Int. J. Mass Spectrom. Ion Processes* **1992**, *112* (1), 93–100.
- (2) Van Vaeck, L.; Adriaens, A.; Gijbels, R. *Mass Spectrom. Rev.* **1999**, *18* (1), 1–47.
- (3) Wu, K. J.; Odom, R. W. *Anal. Chem.* **1996**, *68* (5), 873–882.
- (4) Pour, M. D.; Malmberg, P.; Ewing, A. *Anal. Bioanal. Chem.* **2016**, *408* (12), 3071–3081.
- (5) Altelaar, A. F. M.; van Minnen, J.; Jiménez, C. R.; Heeren, R. M. A.; Piersma, S. R. *Anal. Chem.* **2005**, *77* (3), 735–741.
- (6) Svara, F. N.; Kiss, A.; Jaskolla, T. W.; Karas, M.; Heeren, R. M. A. *Anal. Chem.* **2011**, *83* (21), 8308–8313.
- (7) Dertinger, J. J.; Walker, A. V. *J. Am. Soc. Mass Spectrom.* **2013**, *24* (3), 348–355.
- (8) Fitzgerald, J. J. D.; Kunnath, P.; Walker, A. V. *Anal. Chem.* **2010**, *82* (11), 4413–4419.
- (9) Fisher, G. L.; Bruinen, A. L.; Ogrinc Potočnik, N.; Hammond, J. S.; Bryan, S. R.; Larson, P. E.; Heeren, R. M. A. *Anal. Chem.* **2016**, *88*, 6433.
- (10) Smith, D. F.; Robinson, E. W.; Tolmachev, A. V.; Heeren, R. M. A.; Paša-Tolić, L. *Anal. Chem.* **2011**, *83* (24), 9552–9556.
- (11) Smith, D. F.; Kiss, A.; Leach, F. E., III; Robinson, E. W.; Paša-Tolić, L.; Heeren, R. M. A. *Anal. Bioanal. Chem.* **2013**, *405* (18), 6069–6076.
- (12) MacAleese, L.; Duursma, M. C.; Klerk, L. A.; Fisher, G.; Heeren, R. M. A. *J. Proteomics* **2011**, *74* (7), 993–1001.
- (13) Nygren, H.; Malmberg, P. *Proteomics* **2010**, *10* (8), 1694–1698.
- (14) Yokoyama, Y.; Aoyagi, S.; Fujii, M.; Matsuo, J.; Fletcher, J. S.; Lockyer, N. P.; Vickerman, J. C.; Passarelli, M. K.; Havelund, R.; Seah, M. P. *Anal. Chem.* **2016**, *88* (7), 3592–3597.
- (15) *ProteinProspector*; <http://prospector.ucsf.edu/prospector/mshome.htm> (accessed May 2, 2017).
- (16) Steen, H.; Mann, M. *Nat. Rev. Mol. Cell Biol.* **2004**, *5* (9), 699–711.
- (17) Altelaar, A. F. M.; Taban, I. M.; McDonnell, L. A.; Verhaert, P. D. E. M.; de Lange, R. P. J.; Adan, R. A. H.; Mooi, W. J.; Heeren, R. M. A.; Piersma, S. R. *Int. J. Mass Spectrom.* **2007**, *260* (2–3), 203–211.
- (18) Guenther, S.; Römpf, A.; Kummer, W.; Spengler, B. *Int. J. Mass Spectrom.* **2011**, *305* (2–3), 228–237.
- (19) Calligaris, D.; Feldman, D. R.; Norton, I.; Olubiyi, O.; Changelian, A. N.; Machaidze, R.; Vestal, M. L.; Laws, E. R.; Dunn, I. F.; Santagata, S.; Agar, N. Y. R. *Proc. Natl. Acad. Sci. U. S. A.* **2015**, *112* (32), 9978–9983.
- (20) Chatterji, B.; Dickhut, C.; Mielke, S.; Krüger, J.; Just, I.; Glage, S.; Meier, M.; Wedekind, D.; Pich, A. *Proteomics* **2014**, *14* (13–14), 1674–1687.
- (21) Hanrieder, J.; Ljungdahl, A.; Andersson, M. *J. Visualized Exp.* **2012**, No. 60, e3445.